Received: 8 March 2021 | Revised: 7 June 2021 | Accepted: 26 June 2021

DOI: 10.1002/hbm.25606

RESEARCH ARTICLE

WILEY

Topologically convergent and divergent morphological gray matter networks in early-stage Parkinson's disease with and without mild cognitive impairment

Xueling Suo[1,2,3] | Du Lei[1,2,3,4] | Nannan Li[5] | Junying Li[5] | Jiaxin Peng[5] | Wenbin Li[1,2,3] | Jing Yang[1,2,3] | Kun Qin[1,2,3] | Graham J. Kemp[6] | Rong Peng[5] | Qiyong Gong[1,2,3]

[1]Huaxi MR Research Center (HMRRC), Department of Radiology, West China Hospital of Sichuan University, Chengdu, Sichuan, China

[2]Research Unit of Psychoradiology, Chinese Academy of Medical Sciences, Chengdu, China

[3]Functional and Molecular Imaging Key Laboratory of Sichuan Province, West China Hospital of Sichuan University, Chengdu, China

[4]Department of Psychiatry and Behavioral Neuroscience, University of Cincinnati, Cincinnati, Ohio

[5]Department of Neurology, West China Hospital of Sichuan University, Chengdu, Sichuan, China

[6]Liverpool Magnetic Resonance Imaging Centre (LiMRIC) and Institute of Life Course and Medical Sciences, University of Liverpool, Liverpool, UK

Correspondence
Qiyong Gong and Rong Peng, Huaxi MR Research Center, Department of Radiology, West China Hospital, Sichuan University, No. 37 Guo Xue Xiang, Chengdu, Sichuan 610041, China; Department of Neurology, West China Hospital, Sichuan University, No. 37 Guo Xue Xiang, Chengdu, Sichuan 610041, China.
Email: qiyonggong@hmrrc.org.cn (Q. G.) and qrongpeng@126.com (R. P.)

Funding information
China Postdoctoral Science Foundation, Grant/Award Number: 2020M683317; National Natural Science Foundation of China, Grant/Award Numbers: 81621003, 81820108018, 82001800, 82027808; Post-Doctor Research Project, West China Hospital, Sichuan University, Grant/Award Number: 2019HXBH104; Sichuan Science and Technology Program, Grant/Award Number: 2018HH0077

Abstract

Patients with Parkinson's disease with mild cognitive impairment (PD-M) progress to dementia more frequently than those with normal cognition (PD-N), but the underlying neurobiology remains unclear. This study aimed to define the specific morphological brain network alterations in PD-M, and explore their potential diagnostic value. Twenty-four PD-M patients, 17 PD-N patients, and 29 healthy controls (HC) underwent a structural MRI scan. Similarity between interregional gray matter volume distributions was used to construct individual morphological brain networks. These were analyzed using graph theory and network-based statistics (NBS), and their relationship to neuropsychological tests was assessed. Support vector machine (SVM) was used to perform individual classification. Globally, compared with HC, PD-M showed increased local efficiency ($p = .001$) in their morphological networks, while PD-N showed decreased normalized path length ($p = .008$). Locally, similar nodal deficits were found in the rectus and lingual gyrus, and cerebellum of both PD groups relative to HC; additionally in PD-M nodal deficits involved several frontal and parietal regions, correlated with cognitive scores. NBS found that similar connections were involved in the default mode and cerebellar networks of both PD groups (to a greater extent in PD-M), while PD-M, but not PD-N, showed altered connections involving the frontoparietal network. Using connections identified by NBS, SVM

Xueling Suo and Du Lei contributed equally to this work.

allowed discrimination with high accuracy between PD-N and HC (90%), PD-M and HC (85%), and between the two PD groups (65%). These results suggest that default mode and cerebellar disruption characterizes PD, more so in PD-M, whereas frontoparietal disruption has diagnostic potential.

KEYWORDS
connectome, gray matter, magnetic resonance imaging, mild cognitive impairment, Parkinson's disease, psychoradiology

1 | INTRODUCTION

Patients with Parkinson's disease with mild cognitive impairment (PD-M), who make up 35% of PD patients at diagnosis, progress to dementia more frequently than those with normal cognition (PD-N) (Broeders et al., 2013). PD-M is associated with increased healthcare costs (Vossius, Larsen, Janvin, & Aarsland, 2011), poorer self-reported quality of life (Rosenthal et al., 2010), and greater global disability (Leroi, McDonald, Pantula, & Harbishettar, 2012). Early identification of PD-M in clinical practice would help in planning interventions. However, the neural substrates of PD-M and the factors underlying the transition from PD-N to PD-M are not fully understood. Objective biomarkers are needed that would allow early identification of cognitive deficits in PD.

Neuroimaging studies show that cognitive deficits in PD do not merely involve alterations in discrete brain regions, but are best characterized in terms of altered networks of brain structures (Hall & Lewis, 2019). One theory implicates the disconnection of neural networks in the neurobiology of cognitive deficits in PD (Lang et al., 2019). The concept of the connectome was introduced to define the topology of brain networks (Sporns, Tononi, & Kotter, 2005), and has identified large-scale disconnections in functional and white matter networks in PD-M (Aracil-Bolanos et al., 2019; Baggio et al., 2014; Galantucci et al., 2017; Wang et al., 2020). However, the topology of gray matter (GM) morphological networks remains unclear. What makes this a promising research direction is the growing evidence implicating pathological agents, for example, misfolded proteins, which deposit first in cortical GM (Khairnar et al., 2017) and could induce GM density changes (McMillan & Wolk, 2016), in the development of cognitive decline in PD (Gomperts et al., 2013).

Structural MRI can be used to assess GM networks based on morphological correlations which form a structural covariance network (Bassett et al., 2008; He, Chen, & Evans, 2007; Sanabria-Diaz et al., 2010). A study of interindividual structural covariation in PD-M found disruptions in the parietal and frontal areas (Pereira et al., 2015). While this approach has advanced understanding of brain alterations, it does not provide GM networks for each participant, and thus does not allow analysis of brain–behavior relationships or diagnostic classification at the level of individuals. A recently proposed intraindividual structural covariation method constructs individual networks by computing the morphological similarity relationships of GM (Wang, Jin, Zhang, & Wang, 2016). Studying morphological networks in individuals could improve understanding of the causes and clinical relevance of whole-brain GM network alterations in PD-M, and might provide a noninvasive in vivo biomarker.

This case–control study thus aimed to explore the specific GM brain network alterations in PD-M. As brain network alterations have been implicated in the development of PD-M (Galantucci et al., 2017; Pereira et al., 2015), we hypothesized that the GM network would be abnormal in PD-M compared with PD-N and healthy controls (HC), for example, disrupted nodal centrality in frontoparietal regions. Second, based on the progressive disruptions as cognitive decline worsens (Hassan et al., 2017; Lopes et al., 2017), we expected more widespread topological alterations in PD-M relative to PD-N. Third, we hypothesized that these network alterations would be related to neurocognitive performance in PD-M. Finally, as our recent studies have shown that connectome-wide connectivity can differentiate individuals with brain disorders from HC with high accuracy (Lei et al., 2019; Lei et al., 2020), we expected that GM networks would allow accurate discrimination of PD-M, PD-N, and HC.

2 | MATERIALS AND METHODS

2.1 | Participants

Twenty-four PD-M patients, based on Level II of the recommended Movement Disorder Society (MDS) criteria (Litvan et al., 2012), were recruited from the Movement Disorders Outpatient Unit, West China Hospital of Sichuan Hospital. Seventeen PD-N patients were also recruited to match the demographic and motor features of these. All patients were evaluated either drug-naïve or in an "off" state. Clinical characteristics were assessed by an experienced neurologist. Motor symptom severity was quantified by using the Unified PD Rating Scale motor part (UPDRS-III) (Goetz et al., 2007) and Hoehn and Yahr stage (Goetz et al., 2004). Depression was evaluated by the 24-item version of the Hamilton Depression Scale (HAMD) (Moberg et al., 2001). Diagnostic guidelines in China define Hoehn and Yahr stage ≤2.5 as early-stage PD (Chen et al., 2016). Twenty-nine HC matched for age, gender, and years of education, with no history of neuropsychiatric disease, were recruited for comparative purposes. Details of inclusion and exclusion criteria are described in our previous paper (Suo et al., 2017; Suo et al., 2019; Suo et al., 2021a).

This study was approved by the Ethics Committee of the West China Hospital of Sichuan University. Written informed consent was obtained from all participants before enrollment in the study.

2.2 | Neuropsychological assessments

In the 2 weeks before imaging sessions, each participant underwent neuropsychological assessment with 10 tests (details in Table S1) targeting five cognitive domains (executive function, memory, attention and working memory, visuospatial function, and language) (Litvan et al., 2012), and global cognitive testing with the Mini Mental State Examination (MMSE) and Montreal Cognitive Assessment (MoCA) (Dalrymple-Alford et al., 2010). PD-M was defined as test scores at least 1.5 *SD*s below normative means on at least two neuropsychological tests within five cognitive domains (Litvan et al., 2012). PD-M patients were further divided into cognitive subtypes according to the Task Force criteria: single-domain subtype, with impairment on two tests within only 1 of the 5 cognitive domains; multiple-domain subtype, with impairment on at least 1 test across more than 1 cognitive domains (Cholerton et al., 2014). These were further classified according to which cognitive domains were impaired.

2.3 | Data acquisition and preprocessing

Whole brain 3D T1-weighted images were acquired on a 3.0 T MRI (Siemens Tim Trio, Erlangen, Germany) with the following scanning parameters: echo time 2.3 ms; repetition time 1,900 ms; inversion time 900 ms; field of view 24 × 24 cm^2; matrix size 256 × 256; flip angle 9°; thickness 1.0 mm without gap; 176 slices. During scanning participants lay quietly with eyes closed.

Voxel-based morphometry was applied to the structural MRI images after preprocessing by Statistical Parametric Mapping as previously described (Kong et al., 2015). In brief, we manually checked the raw MRI images to exclude obvious artifacts. Each participant's images were segmented to obtain the GM images, which were converted to the Montreal Neurological Institute stereotactic space. A custom template was created from related tissue segments using the Diffeomorphic Anatomical Registration through Exponential Lie Algebra (DARTEL) tool. The resulting GM images were smoothed individually with a 6 mm full-width at half-maximum Gaussian kernel. Finally, the GM volume (GMV) map was obtained for each participant.

2.4 | Network construction

In graph theory, the two fundamental network elements are nodes and edges. The Automated Anatomical Labeling atlas was used to divide each brain into 116 regions of interest (ROIs) as nodes (Tzourio-Mazoyer et al., 2002), then a Kullback–Leibler divergence-based similarity (KLS) method was used to define interregional connections as edges (Wang et al., 2016). In brief, for each participant, the GMV values of all the voxels in each ROI were extracted, and kernel density estimation was applied to estimate their probability density function, from which the probability distribution function (PDF) was computed. The Kullback–Leibler divergence was computed between each pair of ROIs in their PDFs, then KLS values (ranging from 0 to 1, where 1 represents two identical distributions) were calculated between all possible pairs of brain regions. Finally, the KLS-based 116 × 116 morphological connection matrix was generated for each participant. A wide range of sparsity (*S*) thresholds ($0.05 \le S \le 0.38$ with steps of 0.01) were applied to each matrix to ensure that morphological networks among the three groups had the same number of edges (Zhang et al., 2011).

2.5 | Network analyses

Graph theoretical analyses of GM networks were performed using GRETNA software (Wang et al., 2015). Both global and nodal measures for GM networks were computed at each *S* threshold. *Global network measures* were (a) network integration measures including global efficiency (E_{glob}), characteristic path length (L_p), and normalized characteristic path length (λ); (b) network segregation measures including local efficiency (E_{loc}), clustering coefficient (C_p), and normalized clustering coefficient (γ); and (c) small worldness measure σ (Latora & Marchiori, 2001; Watts & Strogatz, 1998). *Nodal centrality measures* for each node were nodal efficiency, nodal degree, and nodal betweenness (Achard & Bullmore, 2007; Rubinov & Sporns, 2010). Area under the curve (AUC) was computed for each network measure across *S* thresholds to provide a summary measure (Zhang et al., 2011).

2.6 | Statistical analysis

Analysis of variance was used to analyze the continuous variables of demographic and neuropsychological data. Chi-square test was applied to the categorical variables. Clinical assessment between two PD groups was analyzed using two-sample *t* test.

In accordance with a previous study (Ma et al., 2020), nonparametric permutation tests were applied to detect significant differences in the AUC values of network measures among the three groups, and to make post hoc comparisons (for 10,000 permutations). The relationships between network measures that showed significant group differences with neuropsychological tests in each PD group were analyzed using partial correlations, with age, gender, duration, years of education, and UPDRS III as covariates.

The Network-Based Statistic (NBS) toolbox was used to identify specific pairs of regions in which the connections were altered in PD (Zalesky, Fornito, & Bullmore, 2010). Significantly altered components were determined by NBS as significant at $p < .05$ with each connection statistic $F > 5.7$ (by one-way ANOVA test, $p < .005$). Significantly between-group altered components within these connections were then tested, determined by NBS as significant at $p < .05$ with each

connection statistic $T > 3.0$ (by two-sample t-test, $p < .005$). Exploratory support vector machine (SVM) analyses were applied to the connectome-wide connections to determine whether morphological networks can detect PD-M and PD-N at the individual level. Full details of SVM evaluation can be found in our recent paper (Lei et al., 2020).

3 | RESULTS

3.1 | Demographic and clinical characteristics

Significant overall neuropsychological differences were observed among the three groups for MoCA and all specific cognitive measures (all $p < .05$, Table 1) except MMSE, digit span backward, and clock copying tests. LSD posthoc comparisons showed that PD-M performed worse than PD-N and HC on all neuropsychological tests. There was no significant difference in HAMD between PD-M and PD-N.

In PD-M there were four cases (17%) with single-domain impairment (executive function: $N = 2$, memory: $N = 1$, visuospatial function: $N = 1$) and 20 cases (83%) with multiple-domain impairment (1 domains: $N = 9$, 3 domains: $N = 7$, 4 domains: $N = 2$, 5 domains: $N = 2$; attention and working memory: $N = 7$, executive function: $N = 13$, language: $N = 12$, memory: $N = 13$, visuospatial function: $N = 12$). Those with the multiple-domain subtype had a diverse collection of impairments, memory, and executive function being most commonly affected.

TABLE 1 Demographics and clinical characteristics of participants

Variables	HC ($n = 29$)	PD-N ($n = 17$)	PD-M ($n = 24$)	ANOVA p	Posthoc LSD		
					HC vs. PD-N p	HC vs. PD-M p	PD-N vs. PD-M p
Age (years)	52.8 ± 7.7	54.0 ± 8.2	54.3 ± 8.3	.782	.624	.513	.922
Gender (male/female)[a]	12/17	10/7	9/15	.367	.201	.499	.151
Years of education	10.4 ± 3.3	11.4 ± 2.5	9.6 ± 3.4	.239	.307	.413	.092
Age at onset (years)[b]	NA	50.9 ± 8.9	51.0 ± 9.0	—	—	—	.995
Disease duration (years)[b]	NA	2.2 ± 1.6	3.3 ± 2.8	—	—	—	.200
Hoehn and Yahr stage[b]	NA	1.8 ± 0.6	1.9 ± 0.6	—	—	—	.669
Unified PD rating scale III[b]	NA	17.1 ± 9.7	24.3 ± 12.5	—	—	—	.054
Levodopa equivalent daily dose (mg/day)[b]	NA	241 ± 305	291 ± 356	—	—	—	.640
Hamilton depression rating scale	NA	6.1 ± 4.1	8.8 ± 5.1	—	—	—	.081
Mini-mental state examination	28.1 ± 1.5	28.8 ± 1.0	27.7 ± 2.0	.122	.170	.387	.088
Montreal cognitive assessment	22.2 ± 3.5	24.3 ± 2.4	19.3 ± 2.9	**<.001**	.063	**.004**	**<.001**
Attention and working memory							
Digit span backward	4.6 ± 1.6	5.0 ± 1.3	4.3 ± 1.2	.269	.324	.463	.107
Trail making test	48.3 ± 21.1	49.2 ± 11.0	71.3 ± 45.6	**.021**	.925	**.011**	**.028**
Executive function							
Clock drawing test	12.6 ± 1.5	12.5 ± 1.8	10.5 ± 3.3	**.004**	.917	**.003**	**.008**
Verbal fluency test	20.1 ± 5.2	19.7 ± 3.9	15.9 ± 4.6	**.005**	.799	**.003**	**.012**
Language							
Boston naming test	25.1 ± 2.6	26.0 ± 1.5	22.7 ± 3.6	**.001**	.348	**.005**	**.001**
Wechsler adult intelligence scale similarities	16.2 ± 2.7	15.9 ± 3.4	12.3 ± 3.7	**<.001**	.745	**<.001**	**.001**
Memory							
Brief visuospatial memory test–revised	20.6 ± 5.2	22.6 ± 3.6	16.8 ± 5.9	**.002**	.241	**.013**	**.001**
Hopkins verbal learning test	20.5 ± 3.6	22.3 ± 3.6	15.6 ± 4.3	**<.001**	.190	**<.001**	**<.001**
Visuospatial function							
Clock copying test	14.0 ± 1.2	14.1 ± 1.0	13.5 ± 1.1	.174	.954	.098	.124
Judgment of line orientation	22.2 ± 3.9	23.3 ± 3.6	17.2 ± 6.0	**<.001**	.481	**.001**	**<.001**

Note: Data are presented as mean ± *SD*s unless otherwise indicated. $p < 0.05$, shown in bold.

Abbreviations: HC, healthy control; LSD, least significance difference; NA, not available; PD, Parkinson's disease; PD-M, PD with mild cognitive impairment; PD-N, PD with normal cognition.

[a]p value for the gender distribution in the three groups was obtained using a χ^2 test.

[b]p values were obtained using two-sample t tests between PD-N and PD-M.

3.2 | Alterations of global brain network measures

Morphological networks of the three groups showed $\lambda \approx 1$ and $\gamma > 1$ (Figure S1), indicating a small-world organization. There were significant group effects in λ, σ, and E_{loc} among the global network measures of the three groups (Table 2, Figure 1). Posthoc comparisons found that (a) relative to HC, PD-N showed significantly lower λ ($p = .008$) in the brain networks; (b) relative to HC, PD-M showed significantly higher σ ($p = .003$) and E_{loc} ($p = .001$) in the brain networks; and (c) while no significant differences were found between two PD groups in these parameters ($p > .05/3$).

3.3 | Alterations of nodal brain network measures

Brain regions with altered nodal centrality in at least one nodal measure were further localized. Posthoc analysis showed that common to *both PD groups relative to HC* were lower nodal centralities in left lingual gyrus (LING) and right rectus gyrus (REC) with higher nodal centralities in left cerebellum Crus1 and Crus2. Additionally, *in PD-M relative to HC* there were lower nodal centralities in right middle frontal gyrus (MFG), left angular gyrus (ANG) and fusiform gyrus, and higher nodal centralities in right cerebellum 3. Finally, three regions showed significant *differences between the PD groups*, with lower nodal centralities of right paracentral lobe, left inferior frontal gyrus, orbital part, and right superior temporal gyrus (STG) observed in PD-M than PD-N (Table 2, Figure 2).

3.4 | Alterations of morphological connection characteristics

NBS tool was used to identify the disrupted connections in PD (Figure 3). *In PD-N relative to HC*, NBS identified two disconnected subnetworks (Figure 3a). One subnetwork included 7 nodes and 6 decreased connections which mainly encompassed the default mode network regions [bilateral REC, left parahippocampal gyrus (PHG), left precuneus (PCUN), and right Heschl gyrus (HES)], left cerebellum 10, and right amygdala. The second subnetwork included 6 nodes and 5 increased connections centered on cerebellum (Crus1 and 6), which was disconnected with right REC, right postcentral gyrus, right STG, and left inferior occipital gyrus (IOG).

TABLE 2 Gray matter network measures showing significant differences among the PD-M, PD-N, and HC groups

		Posthoc tests		
Measurements	***p*(*F*)**	**HC vs. PD-N*p* (*t*)**	**HC vs. PD-M*p* (*t*)**	**PD-N vs. PD-M*p* (*t*)**
Global				
Normalized characteristic path length	**.045** (3.324)	**.008** (2.470)	.116 (1.229)	.081 (−1.444)
Small-worldness	**.032** (3.657)	.034 (−1.922)	**.003** (−2.844)	.423 (−0.185)
Local efficiency	**.043** (3.243)	.243 (−0.716)	**.001** (−3.024)	.088 (−1.405)
Nodal betweenness				
Right middle frontal gyrus	**.023** (3.857)	.118 (1.182)	**.003** (2.653)	.065 (1.615)
Left fusiform gyrus	**.023** (3.998)	.024 (1.949)	**.010** (2.355)	.433 (0.164)
Left angular gyrus	**.039** (3.423)	.040 (1.738)	**.013** (2.309)	.398 (0.238)
Nodal degree				
Left inferior frontal gyrus, orbital part	**.040** (3.389)	.212 (−0.808)	.027 (1.940)	**.008** (2.504)
Right gyrus rectus	**.038** (3.451)	**.017** (2.180)	**.011** (2.357)	.419 (−0.205)
Left lingual gyrus	**.016** (4.452)	**.015** (2.250)	**.006** (2.641)	.418 (0.236)
Right paracentral lobule	**.037** (3.645)	**.017** (−2.162)	.350 (0.391)	**.002** (3.006)
Right superior temporal gyrus	**.006** (5.532)	.048 (−1.700)	.032 (1.861)	**.001** (3.434)
Left cerebellum Crus1	**.007** (5.281)	**.003** (−2.848)	**.006** (−2.537)	.266 (0.641)
Left cerebellum Crus2	**.032** (3.541)	**.016** (−2.257)	**.008** (−2.548)	.347 (0.386)
Right cerebellum 3	**.031** (3.731)	.167 (−0.993)	**.005** (−2.690)	.090 (−1.388)
Nodal efficiency				
Left inferior frontal gyrus, orbital part	**.035** (3.564)	.098 (−1.306)	.050 (1.686)	**.007** (2.494)
Right superior temporal gyrus	**.010** (4.851)	.037 (−1.777)	.061 (1.590)	**.001** (3.265)
Left cerebellum Crus1	**.002** (6.902)	**.003** (−2.834)	**.001** (−3.084)	.369 (0.363)
Right cerebellum 3	**.024** (3.917)	.054 (−1.656)	**.005** (−2.671)	.201 (−0.865)

Note: Comparisons of global and nodal measures among the three groups ($p < 0.05$, shown in bold) and post hoc pairwise comparisons ($p < 0.05/3$, shown in bold) were performed using nonparametric permutation tests.

Abbreviations: PD, Parkinson's disease; PD-M, PD with mild cognitive impairment; PD-N, PD with normal cognition.

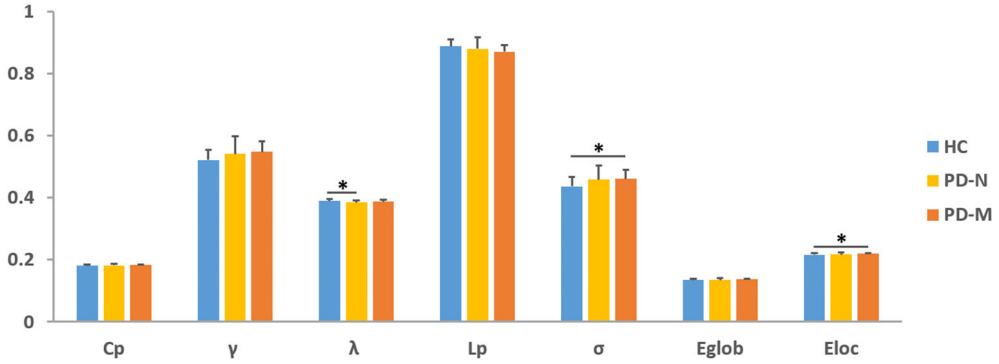

FIGURE 1 Global network properties among the PD-M, PD-N, and HC groups. The bar graph shows the area under the curve of the global network parameters among the 3 groups. Error bars denote *SD*. Black asterisks indicate significant differences in the post hoc comparisons. Abbreviations: PD, Parkinson's disease; PD-M, PD with mild cognitive impairment; PD-N, PD with normal cognition; HC, healthy control; C_p, clustering coefficient; γ, normalized clustering coefficient; L_p, characteristic path length; λ, normalized characteristic path length; E_{loc}, local efficiency; E_{glob}, global efficiency; σ, small-worldness

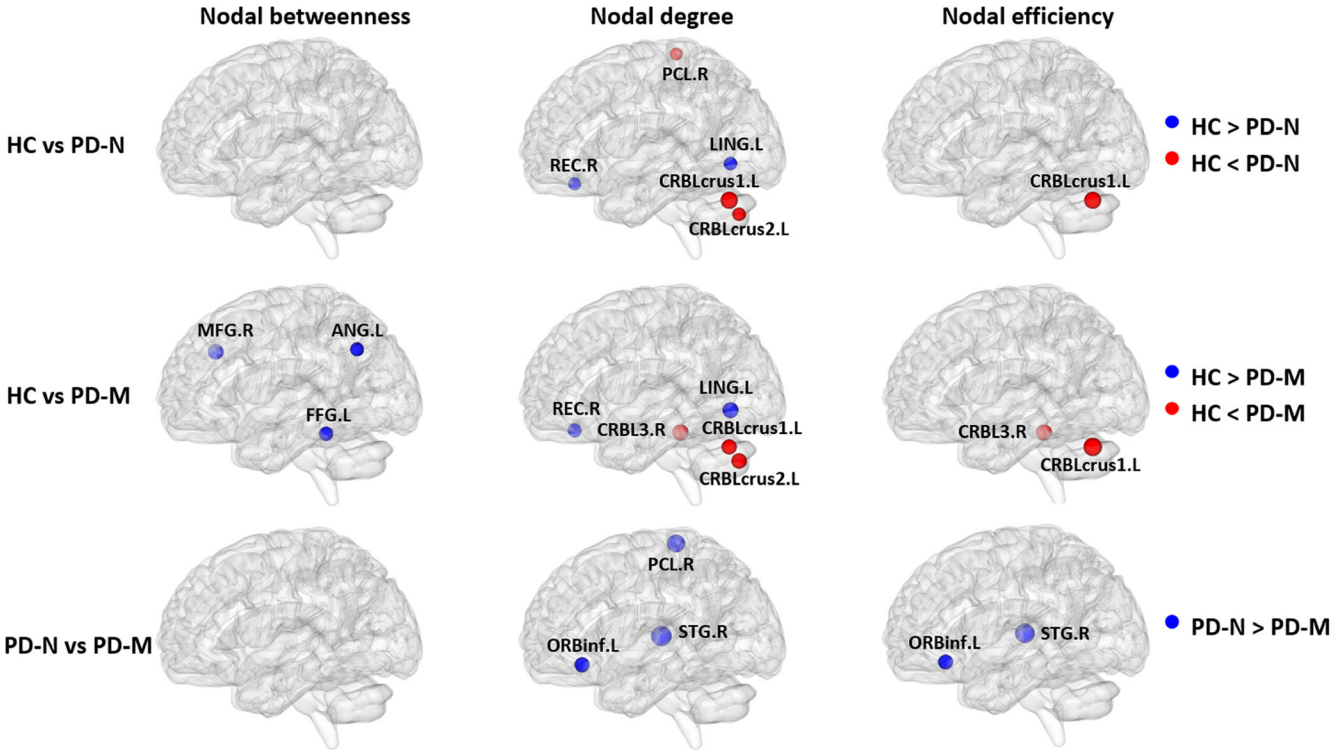

FIGURE 2 Brain regions with significant group effects in the nodal centralities in morphological brain networks compared among the PD-M, PD-N, and HC groups. Node sizes indicating their *T* values are visualized using the BrainNet viewer (http://www.nitrc.org/projects/bnv). The regions are located according to their centroid stereotaxic coordinates. Abbreviations: PD, Parkinson's disease; PD-M, PD with mild cognitive impairment; PD-N, PD with normal cognition; HC, healthy control; ANG, angular gyrus; CRBL, cerebellum; FFG, fusiform gyrus; LING, lingual gyrus; MFG, middle frontal gyrus; ORBinf, inferior frontal gyrus, orbital part; PCL, paracentral lobule; REC, rectus gyrus; STG, superior temporal gyrus; L, left; R, right

In PD-M relative to HC, there were two disconnected subnetworks (Figure 3b). One subnetwork included 11 nodes and 10 decreased connections, which encompassed default mode network (right REC, left medial and posterior cingulate gyrus, right PCUN, right HES, left temporal pole: middle temporal gyrus and right STG), frontal–parietal regions (right supplementary motor area and left superior parietal gyrus), left IOG and left cerebellum 10. The second subnetwork included 8 nodes and 7 increased connections centered on the right REC, which was disconnected with the cerebellum (Crus1, Crus2, 45, 6, and vermis 7).

In PD-M compared with PD-N, there was one disconnected subnetwork comprising 8 regions and 7 decreased connections

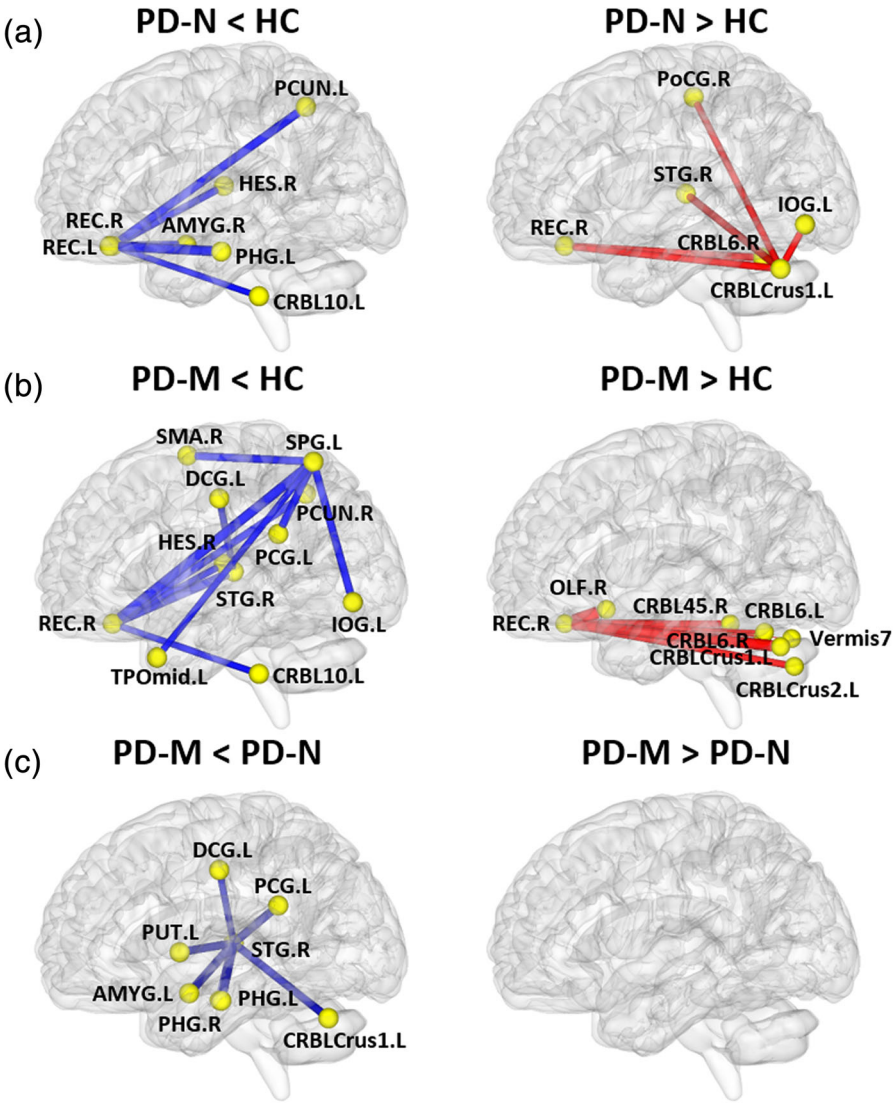

FIGURE 3 The networks showing altered morphological connections compared among the PD-M, PD-N and HC groups. Every node denotes a brain region and every line denotes a connection, mapped onto the cortical surfaces using BrainNet viewer software (www.nitrc.org/projects/bnv/). Red (blue) color represents increased (decreased) morphological connections. Abbreviations: PD, Parkinson's disease; PD-M, PD with mild cognitive impairment; PD-N, PD with normal cognition; HC, healthy control; AMYG, amygdala; CRBL, cerebellum; DCG, median cingulate and paracingulate gyri; HES, Heschl gyrus; IOG, inferior occipital gyrus; OLF, olfactory cortex; PCG, posterior cingulate gyrus; PCUN, precuneus; PHG, parahippocampal gyrus; PoCG, postcentral gyrus; PUT, putamen; REC, rectus gyrus; SMA, supplementary motor area; SPG, superior parietal gyrus; STG, superior temporal gyrus; TPOmid, temporal pole: middle temporal gyrus

(Figure 3c). This subnetwork was centered on right STG, which had decreased connections with left medial and posterior cingulate cortex, PHG, amygdala, putamen, and cerebellum Crus1.

3.5 | Correlations between network measures and neuropsychological variables

For each PD group, correlations between neuropsychological variables and network measures with significant group differences were examined. As shown in Figure 4, in the PD-M group, clock drawing test (CDT) score was positively correlated with nodal betweenness of right MFG ($r = 0.596$, $p = .007$), brief visuospatial memory test-revised (BVMT-R) score was positively correlated with nodal betweenness of left ANG ($r = 0.583$, $p = .009$), and Boston naming test (BNT) score was positively correlated with nodal degree of left cerebellum Crus2 ($r = 0.603$, $p = .006$). In the PD-N group, Wechsler Adult Intelligence Scale-IV (WAIS-IV) similarities score was positively correlated with nodal degree of right STG ($r = 0.754$, $p = .019$). However, these correlations did not survive multiple comparison corrections at false discovery rate < 0.05.

In correlation analyses between network metrics and cognitive tests in the multiple-domain PD-M subtype, our main findings were maintained. Additionally, we found positive correlations between CDT score and E_{loc} ($r = 0.622$, $p = .013$) and nodal degree of left cerebellum Crus2 ($r = 0.519$, $p = .047$) as well as between Judgment of line orientation (JLO) score and nodal degree of left LING ($r = 0.516$, $p = .049$) (Figure S2).

3.6 | Single-subject classification performance

The detailed performance of individual classification is shown in Table S2. Using whole-brain networks, it was only possible to distinguish PD-M from HC with a high mean balanced accuracy (75.2%, $p = .003$). In contrast, using NBS subnetworks, the mean balanced accuracy of three classifications was all above chance (90.0, 85.3, and 64.7% for PD-N vs. HC, PD-M vs. HC, and PD-N vs. PD-M, respectively).

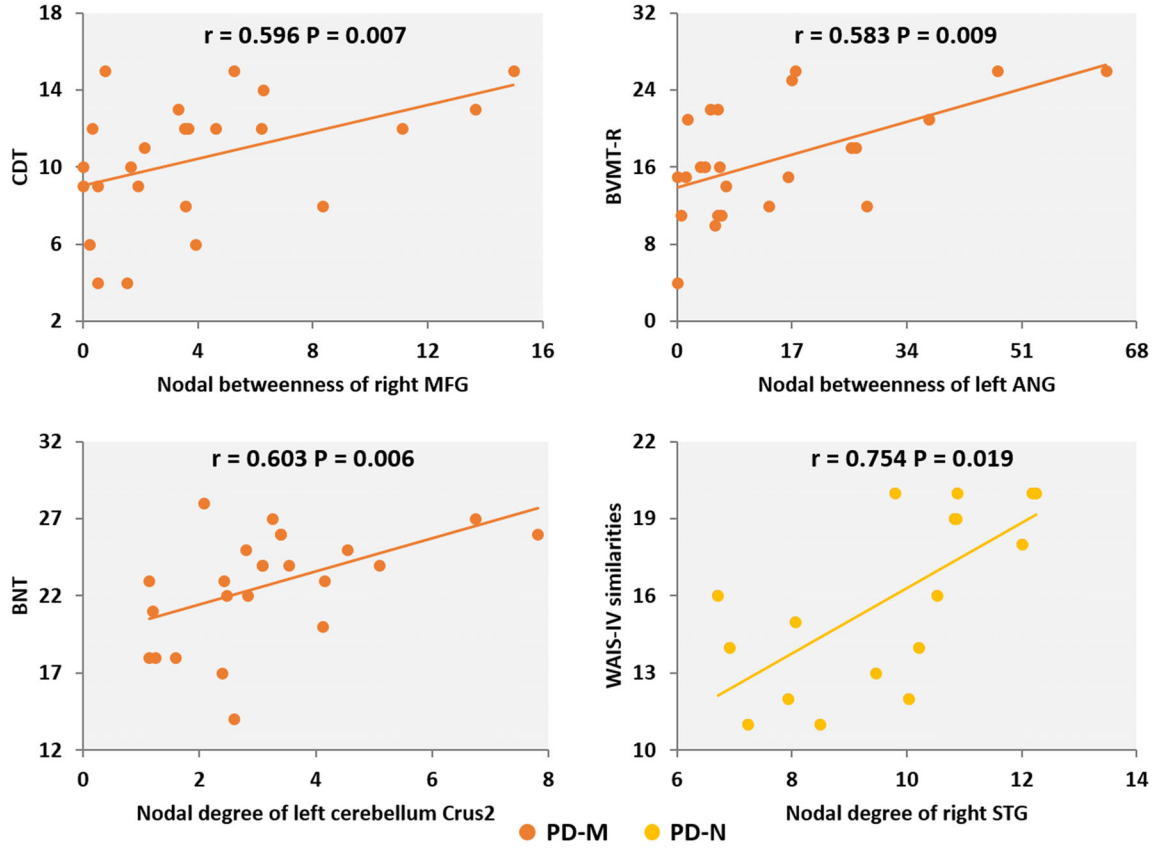

FIGURE 4 The partial correlations between network measures and clinical variables in PD-M and PD-N individuals. Abbreviations: PD, Parkinson's disease; PD-M, PD with mild cognitive impairment; PD-N, PD with normal cognition; ANG, angular gyrus; BVMT-R, brief visuospatial memory test–revised; BNT, Boston naming test; CDT, clock drawing test; MFG, middle frontal gyrus; STG, superior temporal gyrus; WAIS, Wechsler adult intelligence scale; R, right

4 | DISCUSSION

Using structural MRI, we found morphological disruptions of individual brain networks in early-stage PD-M and PD-N. There are five main findings: (a) global network organization in PD was disrupted, as indicated in PD-N by lower λ, and in PD-M by higher E_{loc} and σ; (b) altered nodal centralities in REC, LING, and cerebellum were common to both PD subgroups relative to HC, with additional altered nodal centralities in frontal, parietal and temporal regions in PD-M relative to HC and PD-N; (c) connection deficits of default mode and cerebellar regions were common to both PD subgroups relative to HC, generally to a greater extent in PD-M, while different connections mainly in frontoparietal regions were observed only in PD-M relative to HC; (d) in PD-M positive correlations were observed between nodal betweenness of right MFG and executive function (CDT score), and between nodal betweenness of left ANG and memory (BVMT-R score); (e) this connection analysis permits accurate classifications both between the PD subgroups and HC, and between the PD subgroups. These findings extend the understanding of the neurobiology of cognitive decline in PD, and have potential diagnostic value.

In formal terms, the brain's small-world organization strikes an optimal balance between network segregation (reflected by C_p, γ, and E_{loc}) and integration (reflected by L_p, λ, and E_{glob}) of information processing (Suo et al., 2018). PD-M showed higher network segregation (indicated by higher E_{loc}) compared with HC. A similar network segregation in PD-M (reflected by higher C_p and γ) has been found in previous brain network studies (Baggio et al., 2014; Wang, Mei, et al., 2020). In the present study, PD-M also showed higher network segregation (indicated by higher E_{loc}) relative to HC. These findings taken together suggest that higher network segregation may be more specific to cognitive impairment in PD. However, the higher integration (reflected by lower λ) in early-stage PD-N relative to HC, and the trend toward lower λ in early-stage PD-M relative to HC, were different from that reported for structural networks in early-advanced PD-N or PD-M relative to HC (Galantucci et al., 2017; Pereira et al., 2015). Several factors may contribute to this difference. First, a longitudinal study showed preserved network integration in early-stage PD at baseline, followed by lower network integration over a 4-year follow-up (Olde Dubbelink et al., 2014). This suggests that brain networks in PD may evolve to lower network integration as the disease progresses. Second, there were more elderly (61–80 years) PD participants in these earlier studies, which might contribute to the discrepancy as network integration of structural network is known to decrease with aging (Pereira et al., 2015).

Convergent abnormalities in nodal centralities involving REC and LING were found in both PD subgroups relative to HC, consistent with previous findings in PD (Hou et al., 2018; Zhang, Wang, Liu, Chen, & Liu, 2015). Furthermore, more widespread alterations were observed in PD-M, in line with previous structural findings of additional frontal, temporal, and parietal alterations in PD-M (Beyer, Janvin, Larsen, & Aarsland, 2007; Song et al., 2011; Zhang et al., 2015). Taken together these observations support the idea that the frontal and parietal areas are the substrate responsible for cognitive impairment in PD. Additionally, a positive correlation between the nodal degree of right STG and language (WAIS-IV similarities score) was observed in PD-N. Increased nodal centrality in this region may reflect compensatory improvement in performance, preserving cognition in early cognitively unimpaired PD.

There were similar patterns of reduced connections mainly in the default mode network in both PD subgroups compared with HC. Disrupted default mode network connection is not only related to cognitive deficits in PD-M (Baggio et al., 2015), but also occurs in cognitively unimpaired PD (Tessitore et al., 2012). These findings, with previous reports (Amboni et al., 2015), suggest that default mode network disruption might be a common feature in PD, possibly as a result of neurodegeneration, as in other neurodegenerative disorders (Seeley, Crawford, Zhou, Miller, & Greicius, 2009). Further, compared with PD-N, PD-M showed decreased connections mainly in the temporal areas of default mode network, to a greater extent with increasing levels of cognitive decline. Additionally, PD-M and PD-N showed different connections in the frontoparietal network. Involvement of the frontoparietal networks, and the idea that their disconnection is the substrate of PD-M, has also been suggested on the basis of diffusion and functional MRI studies (Amboni et al., 2015; Galantucci et al., 2017). The network disruptions found in our study are possible morphological correlates of these substrates observed previously in PD-M. Increased morphological connection in the "frontocerebellar loop" may be compensatory (Zhan et al., 2018). Similar observations of disrupted networks have been made in other neurodegenerative disorders such as Alzheimer disease (Mohan et al., 2016; Samson & Claassen, 2017), suggesting a shared profile of neurobiological changes in the cognitive disorders (Pearlson, 2017). Further study is needed of the distinct patterns of network alterations unique to specific neurodegenerative diseases.

Some altered network measures in PD-M were associated with neuropsychological performance. In particularly, positive correlations were observed between nodal betweenness of right MFG and executive function (CDT score), and between nodal betweenness of left ANG and memory (BVMT-R score), which were maintained in the multiple-domain PD-M subtype. Additional positive correlation between nodal degree of left LING and visuospatial function (JLO score) was observed in the multiple-domain PD-M subtype. Previous studies have found positive correlations between executive function performance and dopaminergic activity/synaptic density in the MFG (Andersen et al., 2021; Picco et al., 2015); furthermore, atrophy, hypometabolism, and hypoactivity in the occipito-parietal areas associated with cognitive dysfunction in PD (Gonzalez-Redondo et al., 2014; Guo et al., 2021; Pagonabarraga et al., 2013). All these findings help explain why impairment of frontal/executive and posterior cortical/memory and visuospatial functions are frequent neuropsychological features in PD-M (Lin & Wu, 2015). Notably, PD individuals with visuospatial and memory deficits (posterior cortical deficits) had an increased risk of progression to dementia (Williams-Gray et al., 2009). Interestingly, we found correlations between cerebellum and language (BNT score) in all PD-M as well as with executive function (CDT score) in the multiple-domain PD-M subtype. Recent evidence implicates the cerebellum in the control of several cognitive processes including in memory and language (Stoodley, 2012). Our results, consistent with these reports, support the PD-related cognitive pattern characterized by metabolic reductions in frontal and parietal regions and increases in cerebellum (Huang et al., 2007).

Lastly, consistent with our final hypothesis, the exploratory SVM classification analyses showed that NBS subnetworks could not only differentiate PD-M and PD-N from HC, but also between PD-M and PD-N at an individual level with significant above-chance accuracy. Our structural results, combined with previous functional findings (Lei et al., 2019), support the emerging view that network connections may be a powerful tool to characterize brain disorders at the individual level. Although machine learning is not yet available in day-to-day clinical practice, in light of the urgent clinical need for objective biomarkers in the early stage of the disease, it has the potential to inform the development of diagnostic imaging-based markers. Future studies could explore whether our findings are specific to PD or trans-diagnostic features of neurologic disorders. The accuracy of the SVM classification between PD-M and PD-N was not particularly high, and better classification performance may be achieved via other advanced models such as deep learning, although computation involving large numbers of parameters will require a larger sample size (Vieira, Pinaya, & Mechelli, 2017).

Our study has some limitations. First, it was cross-sectional; longitudinal studies are needed to investigate how these network disruptions evolve with the progression of cognitive deterioration. Second, the sample size is not large, which may be why the results of correlation analyses between network metrics and clinical variables did not survive multiple-comparison correction. However, our main findings are comparable to studies with large or multicenter PD-M cohorts that also used the MDS Task Force criteria, in which most PD-M showed multiple-domain deficits (Cholerton et al., 2014; Kalbe et al., 2016). Our finding are in some contrast to older studies reporting greater single-domain impairments (Litvan et al., 2011); the differences may be related to cohort characteristics (e.g., early vs. late-stage PD) and the definition of PD-M (e.g., whether the cut-off scores are taken as 1 or 1.5 *SD*s below normative means). There is substantial heterogeneity in cognitive subdomain deficits in PD-M. Full study of the different subtype profiles will require a stratified statistical analysis which is beyond the scope of the current study, although it is a focus of our ongoing work. Third, the individual brain networks were constructed on the basis of the similarities between interregional GM volume distributions. Other morphological features could also be considered for calculating network metrics (Li et al., 2021), and it will be interesting to explore different types of GM networks for comprehensively mapping cognitive impairment in PD. Fourth, depression is reportedly associated with PD-M, although this has not reached statistical significance in all studies (Baiano, Barone, Trojano, & Santangelo, 2020). Some neurobiological changes in brain circuits are common to PD-M and

other causes of neuropsychiatric symptoms, and these may play an important role in the complex relationship between cognitive impairment and psychiatric symptoms in PD (Petkus et al., 2020), which deserves further study.

In conclusion, this study shows both convergent and divergent disruptions of morphological network organization in PD-M and PD-N. Disrupted network segregation and frontoparietal regions in GM morphological networks were associated with cognitive impairment in PD. Furthermore, connectome-wide connections showed potential single-subject discriminative value between each PD group and HC as well as between PD-M and PD-N. Disrupted morphological networks may contribute to the pathophysiology, and have promise as potential neuroimaging biomarkers for the early diagnosis of cognitive impairment in PD. Specifically, this study adds to the field of psychoradiology (Gong, Kendrick, & Lu, 2021; Lan et al., 2021; Pan et al., 2021; Suo et al., 2021b; Wang et al., 2020), an evolving subspecialty of radiology, which is primed to be of major clinical importance in guiding diagnostic and therapeutic decision making in patients with neuropsychiatric disorders.

ACKNOWLEDGMENTS

This research has received funding from the National Natural Science Foundation (Grant Nos. 81621003, 81820108018, 82001800 and 82027808), the Sichuan Science and Technology Program (Grant No. 2018HH0077), the China Postdoctoral Science Foundation (Grant No. 2020M683317), and the Post-Doctor Research Project, West China Hospital, Sichuan University (Grant No. 2019HXBH104).

CONFLICT OF INTEREST

None of the authors have financial conflicts of interest.

DATA AVAILABILITY STATEMENT

The data that support the findings of this study are available from the corresponding authors upon reasonable request.

ORCID

Rong Peng https://orcid.org/0000-0002-0373-6035
Qiyong Gong https://orcid.org/0000-0002-5912-4871

REFERENCES

Achard, S., & Bullmore, E. (2007). Efficiency and cost of economical brain functional networks. *PLoS Computational Biology*, *3*, e17. https://doi.org/10.1371/journal.pcbi.0030017

Amboni, M., Tessitore, A., Esposito, F., Santangelo, G., Picillo, M., Vitale, C., … Barone, P. (2015). Resting-state functional connectivity associated with mild cognitive impairment in Parkinson's disease. *Journal of Neurology*, *262*, 425–434. https://doi.org/10.1007/s00415-014-7591-5

Andersen, K. B., Hansen, A. K., Damholdt, M. F., Horsager, J., Skjaerbaek, C., Gottrup, H., … Borghammer, P. (2021). Reduced synaptic density in patients with Lewy body dementia: An [C-11]UCB-J PET imaging study. *Movement Disorders*. https://doi.org/10.1002/mds.28617

Aracil-Bolanos, I., Sampedro, F., Marin-Lahoz, J., Horta-Barba, A., Martinez-Horta, S., Boti, M., … Pagonabarraga, J. (2019). A divergent breakdown of neurocognitive networks in Parkinson's disease mild cognitive impairment. *Human Brain Mapping*, *40*, 3233–3242. https://doi.org/10.1002/hbm.24593

Baggio, H. C., Sala-Llonch, R., Segura, B., Marti, M. J., Valldeoriola, F., Compta, Y., … Junque, C. (2014). Functional brain networks and cognitive deficits in Parkinson's disease. *Human Brain Mapping*, *35*, 4620–4634. https://doi.org/10.1002/hbm.22499

Baggio, H. C., Segura, B., Sala-Llonch, R., Marti, M. J., Valldeoriola, F., Compta, Y., … Junque, C. (2015). Cognitive impairment and resting-state network connectivity in Parkinson's disease. *Human Brain Mapping*, *36*, 199–212. https://doi.org/10.1002/hbm.22622

Baiano, C., Barone, P., Trojano, L., & Santangelo, G. (2020). Prevalence and clinical aspects of mild cognitive impairment in Parkinson's disease: A meta-analysis. *Movement Disorders*, *35*, 45–54. https://doi.org/10.1002/mds.27902

Bassett, D. S., Bullmore, E., Verchinski, B. A., Mattay, V. S., Weinberger, D. R., & Meyer-Lindenberg, A. (2008). Hierarchical organization of human cortical networks in health and schizophrenia. *The Journal of Neuroscience*, *28*, 9239–9248. https://doi.org/10.1523/JNEUROSCI.1929-08.2008

Beyer, M. K., Janvin, C. C., Larsen, J. P., & Aarsland, D. (2007). A magnetic resonance imaging study of patients with Parkinson's disease with mild cognitive impairment and dementia using voxel-based morphometry. *Journal of Neurology, Neurosurgery, and Psychiatry*, *78*, 254–259. https://doi.org/10.1136/jnnp.2006.093849

Broeders, M., de Bie, R. M., Velseboer, D. C., Speelman, J. D., Muslimovic, D., & Schmand, B. (2013). Evolution of mild cognitive impairment in Parkinson disease. *Neurology*, *81*, 346–352. https://doi.org/10.1212/WNL.0b013e31829c5c86

Chen, S., Chan, P., Sun, S., Chen, H., Zhang, B., Le, W., … Xiao, Q. (2016). The recommendations of Chinese Parkinson's disease and movement disorder society consensus on therapeutic management of Parkinson's disease. *Translational Neurodegeneration*, *5*, 12. https://doi.org/10.1186/s40035-016-0059-z

Cholerton, B. A., Zabetian, C. P., Wan, J. Y., Montine, T. J., Quinn, J. F., Mata, I. F., … Edwards, K. L. (2014). Evaluation of mild cognitive impairment subtypes in Parkinson's disease. *Movement Disorders*, *29*, 756–764. https://doi.org/10.1002/mds.25875

Dalrymple-Alford, J. C., MacAskill, M. R., Nakas, C. T., Livingston, L., Graham, C., Crucian, G. P., … Anderson, T. J. (2010). The MoCA: Well-suited screen for cognitive impairment in Parkinson disease. *Neurology*, *75*, 1717–1725. https://doi.org/10.1212/WNL.0b013e3181fc29c9

Galantucci, S., Agosta, F., Stefanova, E., Basaia, S., van den Heuvel, M. P., Stojkovic, T., … Filippi, M. (2017). Structural brain connectome and cognitive impairment in Parkinson disease. *Radiology*, *283*, 515–525. https://doi.org/10.1148/radiol.2016160274

Goetz, C. G., Fahn, S., Martinez-Martin, P., Poewe, W., Sampaio, C., Stebbins, G. T., … LaPelle, N. (2007). Movement Disorder Society-sponsored revision of the unified Parkinson's disease rating scale (MDS-UPDRS): Process, format, and clinimetric testing plan. *Movement Disorders*, *22*, 41–47. https://doi.org/10.1002/mds.21198

Goetz, C. G., Poewe, W., Rascol, O., Sampaio, C., Stebbins, G. T., Counsell, C., … Movement Disorder Society Task Force on Rating Scales for Parkinson's Disease. (2004). Movement disorder society task force report on the Hoehn and Yahr staging scale: Status and recommendations. *Movement Disorders*, *19*, 1020–1028. https://doi.org/10.1002/mds.20213

Gomperts, S. N., Locascio, J. J., Rentz, D., Santarlasci, A., Marquie, M., Johnson, K. A., & Growdon, J. H. (2013). Amyloid is linked to cognitive decline in patients with Parkinson disease without dementia. *Neurology*, *80*, 85–91. https://doi.org/10.1212/WNL.0b013e31827b1a07

Gong, Q., Kendrick, K. M., & Lu, L. (2021). Psychoradiology: A new era for neuropsychiatric imaging. *Psychoradiology*, *1*, 1–2. https://doi.org/10.1093/psyrad/kkaa001

Gonzalez-Redondo, R., Garcia-Garcia, D., Clavero, P., Gasca-Salas, C., Garcia-Eulate, R., Zubieta, J. L., … Rodriguez-Oroz, M. C. (2014). Grey matter hypometabolism and atrophy in Parkinson's disease with cognitive impairment: A two-step process. *Brain*, *137*, 2356–2367. https://doi.org/10.1093/brain/awu159

Guo, W. N., Jin, W., Li, N., Gao, J. S., Wang, J. X., Chang, Y. J., … Wang, T. J. (2021). Brain activity alterations in patients with Parkinson's disease with cognitive impairment based on resting-state functional MRI. *Neuroscience Letters*, *747*, 135672. https://doi.org/10.1016/J.Neulet.2021.135672

Hall, J. M., & Lewis, S. J. G. (2019). Neural correlates of cognitive impairment in Parkinson's disease: A review of structural MRI findings. *International Review of Neurobiology*, *144*, 1–28. https://doi.org/10.1016/bs.irn.2018.09.009

Hassan, M., Chaton, L., Benquet, P., Delval, A., Leroy, C., Plomhause, L., … Dujardin, K. (2017). Functional connectivity disruptions correlate with cognitive phenotypes in Parkinson's disease. *Neuroimage: Clinical*, *14*, 591–601. https://doi.org/10.1016/j.nicl.2017.03.002

He, Y., Chen, Z. J., & Evans, A. C. (2007). Small-world anatomical networks in the human brain revealed by cortical thickness from MRI. *Cerebral Cortex*, *17*, 2407–2419. https://doi.org/10.1093/cercor/bhl149

Hou, Y., Wei, Q., Ou, R., Yang, J., Song, W., Gong, Q., & Shang, H. (2018). Impaired topographic organization in cognitively unimpaired drug-naive patients with rigidity-dominant Parkinson's disease. *Parkinsonism & Related Disorders*, *56*, 52–57. https://doi.org/10.1016/j.parkreldis.2018.06.021

Huang, C. R., Mattis, P., Tang, C. K., Perrine, K., Carbon, M., & Eidelberg, D. (2007). Metabolic brain networks associated with cognitive function in Parkinson's disease. *NeuroImage*, *34*, 714–723. https://doi.org/10.1016/j.neuroimage.2006.09.003

Kalbe, E., Rehberg, S. P., Heber, I., Kronenbuerger, M., Schulz, J. B., Storch, A., … Dodel, R. (2016). Subtypes of mild cognitive impairment in patients with Parkinson's disease: Evidence from the LANDSCAPE study. *Journal of Neurology, Neurosurgery, and Psychiatry*, *87*, 1099–1105. https://doi.org/10.1136/jnnp-2016-313838

Khairnar, A., Ruda-Kucerova, J., Szabo, N., Drazanova, E., Arab, A., Hutter-Paier, B., … Rektorova, I. (2017). Early and progressive microstructural brain changes in mice overexpressing human alpha-Synuclein detected by diffusion kurtosis imaging. *Brain, Behavior, and Immunity*, *61*, 197–208. https://doi.org/10.1016/j.bbi.2016.11.027

Kong, X. Z., Liu, Z., Huang, L., Wang, X., Yang, Z., Zhou, G., … Liu, J. (2015). Mapping individual brain networks using statistical similarity in regional morphology from MRI. *PLoS One*, *10*, e0141840. https://doi.org/10.1371/journal.pone.0141840

Lan, H., Suo, X. L., Li, W. B., Li, N. N., Li, J. Y., Peng, J. X., … Gong, Q. Y. (2021). Abnormalities of intrinsic brain activity in essential tremor: A meta-analysis of resting-state functional imaging. *Human Brain Mapping*, *42*, 3156–3167. https://doi.org/10.1002/hbm.25425

Lang, S., Hanganu, A., Gan, L. S., Kibreab, M., Auclair-Ouellet, N., Alrazi, T., … Monchi, O. (2019). Network basis of the dysexecutive and posterior cortical cognitive profiles in Parkinson's disease. *Movement Disorders*, *34*, 893–902. https://doi.org/10.1002/mds.27674

Latora, V., & Marchiori, M. (2001). Efficient behavior of small-world networks. *Physical Review Letters*, *87*, 198701. https://doi.org/10.1103/PhysRevLett.87.198701

Lei, D., Pinaya, W. H. L., van Amelsvoort, T., Marcelis, M., Donohoe, G., Mothersill, D. O., … Mechelli, A. (2019). Detecting schizophrenia at the level of the individual: Relative diagnostic value of whole-brain images, connectome-wide functional connectivity and graph-based metrics. *Psychological Medicine*, *50*, 1–10. https://doi.org/10.1017/S0033291719001934

Lei, D., Pinaya, W. H. L., Young, J., van Amelsvoort, T., Marcelis, M., Donohoe, G., … Mechelli, A. (2020). Integrating machining learning and multimodal neuroimaging to detect schizophrenia at the level of the individual. *Human Brain Mapping*, *41*, 1119–1135. https://doi.org/10.1002/hbm.24863

Leroi, I., McDonald, K., Pantula, H., & Harbishettar, V. (2012). Cognitive impairment in Parkinson disease: Impact on quality of life, disability, and caregiver burden. *Journal of Geriatric Psychiatry and Neurology*, *25*, 208–214. https://doi.org/10.1177/0891988712464823

Li, Y., Wang, N., Wang, H., Lv, Y., Zou, Q., & Wang, J. (2021). Surface-based single-subject morphological brain networks: Effects of morphological index, brain parcellation and similarity measure, sample size-varying stability and test-retest reliability. *NeuroImage*, *235*, 118018. https://doi.org/10.1016/j.neuroimage.2021.118018

Lin, C. H., & Wu, R. M. (2015). Biomarkers of cognitive decline in Parkinson's disease. *Parkinsonism & Related Disorders*, *21*, 431–443. https://doi.org/10.1016/j.parkreldis.2015.02.010

Litvan, I., Aarsland, D., Adler, C. H., Goldman, J. G., Kulisevsky, J., Mollenhauer, B., … Weintraub, D. (2011). MDS task force on mild cognitive impairment in Parkinson's disease: Critical review of PD-MCI. *Movement Disorders*, *26*, 1814–1824. https://doi.org/10.1002/mds.23823

Litvan, I., Goldman, J. G., Troster, A. I., Schmand, B. A., Weintraub, D., Petersen, R. C., … Emre, M. (2012). Diagnostic criteria for mild cognitive impairment in Parkinson's disease: Movement Disorder Society Task Force guidelines. *Movement Disorders*, *27*, 349–356. https://doi.org/10.1002/mds.24893

Lopes, R., Delmaire, C., Defebvre, L., Moonen, A. J., Duits, A. A., Hofman, P., … Dujardin, K. (2017). Cognitive phenotypes in Parkinson's disease differ in terms of brain-network organization and connectivity. *Human Brain Mapping*, *38*, 1604–1621. https://doi.org/10.1002/hbm.23474

Ma, Q., Tang, Y., Wang, F., Liao, X., Jiang, X., Wei, S., … Xia, M. (2020). Transdiagnostic dysfunctions in brain modules across patients with schizophrenia, bipolar disorder, and major depressive disorder: A connectome-based study. *Schizophrenia Bulletin*, *46*, 699–712. https://doi.org/10.1093/schbul/sbz111

McMillan, C. T., & Wolk, D. A. (2016). Presence of cerebral amyloid modulates phenotype and pattern of neurodegeneration in early Parkinson's disease. *Journal of Neurology, Neurosurgery, and Psychiatry*, *87*, 1112–1122. https://doi.org/10.1136/jnnp-2015-312690

Moberg, P. J., Lazarus, L. W., Mesholam, R. I., Bilker, W., Chuy, I. L., Neyman, I., & Markvart, V. (2001). Comparison of the standard and structured interview guide for the Hamilton depression rating scale in depressed geriatric inpatients. *The American Journal of Geriatric Psychiatry*, *9*, 35–40. https://doi.org/10.1176/appi.ajgp.9.1.35

Mohan, A., Roberto, A. J., Mohan, A., Lorenzo, A., Jones, K., Carney, M. J., … Lapidus, K. A. B. (2016). The significance of the default mode network (DMN) in neurological and neuropsychiatric disorders: A review. *The Yale Journal of Biology and Medicine*, *89*, 49–57.

Olde Dubbelink, K. T., Hillebrand, A., Stoffers, D., Deijen, J. B., Twisk, J. W., Stam, C. J., & Berendse, H. W. (2014). Disrupted brain network topology in Parkinson's disease: A longitudinal magnetoencephalography study. *Brain*, *137*, 197–207. https://doi.org/10.1093/brain/awt316

Pagonabarraga, J., Corcuera-Solano, I., Vives-Gilabert, Y., Llebaria, G., Garcia-Sanchez, C., Pascual-Sedano, B., … Gomez-Anson, B. (2013). Pattern of regional cortical thinning associated with cognitive deterioration in Parkinson's disease. *Plos One*, *8*(1), e54980. https://doi.org/10.1371/journal.pone.0054980

Pan, N. F., Wang, S., Zhao, Y. J., Lai, H., Qin, K., Li, J. G., … Gong, Q. Y. (2021). Brain gray matter structures associated with trait impulsivity: A systematic review and voxel-based meta-analysis. *Human Brain Mapping*, *42*, 2214–2235. https://doi.org/10.1002/hbm.25361

Pearlson, G. D. (2017). Applications of resting state functional MR imaging to neuropsychiatric diseases. *Neuroimaging Clinics of North America*, *27*, 709–723. https://doi.org/10.1016/j.nic.2017.06.005

Pereira, J. B., Aarsland, D., Ginestet, C. E., Lebedev, A. V., Wahlund, L. O., Simmons, A., … Westman, E. (2015). Aberrant cerebral network topology and mild cognitive impairment in early Parkinson's disease. *Human Brain Mapping*, *36*, 2980–2995. https://doi.org/10.1002/hbm.22822

Petkus, A. J., Filoteo, J. V., Schiehser, D. M., Gomez, M. E., Hui, J. S., Jarrahi, B., … Petzinger, G. M. (2020). Mild cognitive impairment, psychiatric symptoms, and executive functioning in patients with Parkinson's disease. *International Journal of Geriatric Psychiatry*, *35*, 396–404. https://doi.org/10.1002/gps.5255

Picco, A., Morbelli, S., Piccardo, A., Arnaldi, D., Girtler, N., Brugnolo, A., … Nobili, F. (2015). Brain (18)F-DOPA PET and cognition in de novo Parkinson's disease. *European Journal of Nuclear Medicine and Molecular Imaging*, *42*, 1062–1070. https://doi.org/10.1007/s00259-015-3039-0

Rosenthal, E., Brennan, L., Xie, S., Hurtig, H., Milber, J., Weintraub, D., … Siderowf, A. (2010). Association between cognition and function in patients with Parkinson disease with and without dementia. *Movement Disorders*, *25*, 1170–1176. https://doi.org/10.1002/mds.23073

Rubinov, M., & Sporns, O. (2010). Complex network measures of brain connectivity: Uses and interpretations. *NeuroImage*, *52*, 1059–1069. https://doi.org/10.1016/j.neuroimage.2009.10.003

Samson, M., & Claassen, D. O. (2017). Neurodegeneration and the cerebellum. *Neurodegenerative Diseases*, *17*, 155–165. https://doi.org/10.1159/000460818

Sanabria-Diaz, G., Melie-Garcia, L., Iturria-Medina, Y., Aleman-Gomez, Y., Hernandez-Gonzalez, G., Valdes-Urrutia, L., … Valdes-Sosa, P. (2010). Surface area and cortical thickness descriptors reveal different attributes of the structural human brain networks. *NeuroImage*, *50*, 1497–1510. https://doi.org/10.1016/j.neuroimage.2010.01.028

Seeley, W. W., Crawford, R. K., Zhou, J., Miller, B. L., & Greicius, M. D. (2009). Neurodegenerative diseases target large-scale human brain networks. *Neuron*, *62*, 42–52. https://doi.org/10.1016/j.neuron.2009.03.024

Song, S. K., Lee, J. E., Park, H. J., Sohn, Y. H., Lee, J. D., & Lee, P. H. (2011). The pattern of cortical atrophy in patients with Parkinson's disease according to cognitive status. *Movement Disorders*, *26*, 289–296. https://doi.org/10.1002/mds.23477

Sporns, O., Tononi, G., & Kotter, R. (2005). The human connectome: A structural description of the human brain. *PLoS Computational Biology*, *1*, e42. https://doi.org/10.1371/journal.pcbi.0010042

Stoodley, C. J. (2012). The cerebellum and cognition: Evidence from functional imaging studies. *Cerebellum*, *11*, 352–365. https://doi.org/10.1007/s12311-011-0260-7

Suo, X., Lei, D., Cheng, L., Li, N., Zuo, P., Wang, D. J. J., … Gong, Q. (2019). Multidelay multiparametric arterial spin labeling perfusion MRI and mild cognitive impairment in early stage Parkinson's disease. *Human Brain Mapping*, *40*, 1317–1327. https://doi.org/10.1002/hbm.24451

Suo, X., Lei, D., Li, L., Li, W., Dai, J., Wang, S., … Gong, Q. (2018). Psychoradiological patterns of small-world properties and a systematic review of connectome studies of patients with 6 major psychiatric disorders. *Journal of Psychiatry & Neuroscience*, *43*, 170214–170427. https://doi.org/10.1503/jpn.170214

Suo, X., Lei, D., Li, N., Cheng, L., Chen, F., Wang, M., … Gong, Q. (2017). Functional brain connectome and its relation to Hoehn and Yahr stage in Parkinson disease. *Radiology*, *285*, 904–913. https://doi.org/10.1148/radiol.2017162929

Suo, X., Lei, D., Li, N., Li, W., Kemp, G. J., Sweeney, J. A., … Gong, Q. (2021a). Disrupted morphological grey matter networks in early-stage Parkinson's disease. *Brain Structure & Function*, *226*, 1389–1403. https://doi.org/10.1007/s00429-020-02200-9

Suo, X., Lei, D., Li, W., Li, L., Dai, J., Wang, S., … Gong, Q. (2021b). Altered white matter microarchitecture in Parkinson's disease: A voxel-based meta-analysis of diffusion tensor imaging studies. *Frontiers of Medicine*, *15*, 125–138. https://doi.org/10.1007/s11684-019-0725-5

Tessitore, A., Esposito, F., Vitale, C., Santangelo, G., Amboni, M., Russo, A., … Tedeschi, G. (2012). Default-mode network connectivity in cognitively unimpaired patients with Parkinson disease. *Neurology*, *79*, 2226–2232. https://doi.org/10.1212/WNL.0b013e31827689d6

Tzourio-Mazoyer, N., Landeau, B., Papathanassiou, D., Crivello, F., Etard, O., Delcroix, N., … Joliot, M. (2002). Automated anatomical labeling of activations in SPM using a macroscopic anatomical parcellation of the MNI MRI single-subject brain. *NeuroImage*, *15*, 273–289. https://doi.org/10.1006/nimg.2001.0978

Vieira, S., Pinaya, W. H. L., & Mechelli, A. (2017). Using deep learning to investigate the neuroimaging correlates of psychiatric and neurological disorders: Methods and applications. *Neuroscience and Biobehavioral Reviews*, *74*, 58–75. https://doi.org/10.1016/j.neubiorev.2017.01.002

Vossius, C., Larsen, J. P., Janvin, C., & Aarsland, D. (2011). The economic impact of cognitive impairment in Parkinson's disease. *Movement Disorders*, *26*, 1541–1544. https://doi.org/10.1002/mds.23661

Wang, H., Jin, X., Zhang, Y., & Wang, J. (2016). Single-subject morphological brain networks: Connectivity mapping, topological characterization and test-retest reliability. *Brain and Behavior: A Cognitive Neuroscience Perspective*, *6*, e00448. https://doi.org/10.1002/brb3.448

Wang, J., Wang, X., Xia, M., Liao, X., Evans, A., & He, Y. (2015). GRETNA: A graph theoretical network analysis toolbox for imaging connectomics. *Frontiers in Human Neuroscience*, *9*, 386. https://doi.org/10.3389/fnhum.2015.00386

Wang, S., Zhao, Y. J., Li, J. G., Lai, H., Qiu, C., Pan, N. F., & Gong, Q. Y. (2020). Neurostructural correlates of hope: Dispositional hope mediates the impact of the SMA gray matter volume on subjective well-being in late adolescence. *Social Cognitive and Affective Neuroscience*, *15*, 395–404. https://doi.org/10.1093/scan/nsaa046

Wang, W., Mei, M., Gao, Y., Huang, B., Qiu, Y., Zhang, Y., … Nie, K. (2020). Changes of brain structural network connection in Parkinson's disease patients with mild cognitive dysfunction: A study based on diffusion tensor imaging. *Journal of Neurology*, *267*, 933–943. https://doi.org/10.1007/s00415-019-09645-x

Watts, D. J., & Strogatz, S. H. (1998). Collective dynamics of "small-world" networks. *Nature*, *393*, 440–442. https://doi.org/10.1038/30918

Williams-Gray, C. H., Evans, J. R., Goris, A., Foltynie, T., Ban, M., Robbins, T. W., … Barker, R. A. (2009). The distinct cognitive syndromes of Parkinson's disease: 5 year follow-up of the CamPalGN cohort. *Brain*, *132*, 2958–2969. https://doi.org/10.1093/brain/awp245

Zalesky, A., Fornito, A., & Bullmore, E. T. (2010). Network-based statistic: Identifying differences in brain networks. *NeuroImage*, *53*, 1197–1207. https://doi.org/10.1016/j.neuroimage.2010.06.041

Zhan, Z. W., Lin, L. Z., Yu, E. H., Xin, J. W., Lin, L., Lin, H. L., … Pan, X. D. (2018). Abnormal resting-state functional connectivity in posterior cingulate cortex of Parkinson's disease with mild cognitive impairment and dementia. *CNS Neuroscience & Therapeutics*, *24*, 897–905. https://doi.org/10.1111/cns.12838

Zhang, D., Wang, J., Liu, X., Chen, J., & Liu, B. (2015). Aberrant brain network efficiency in Parkinson's disease patients with tremor: A multimodality study. *Frontiers in Aging Neuroscience*, *7*, 169. https://doi.org/10.3389/fnagi.2015.00169

Zhang, J., Wang, J., Wu, Q., Kuang, W., Huang, X., He, Y., & Gong, Q. (2011). Disrupted brain connectivity networks in drug-naive, first-episode major depressive disorder. *Biological Psychiatry*, *70*, 334–342. https://doi.org/10.1016/j.biopsych.2011.05.018

Zhang, J., Zhang, Y. T., Hu, W. D., Li, L., Liu, G. Y., & Bai, Y. P. (2015). Gray matter atrophy in patients with Parkinson's disease and those with mild cognitive impairment: A voxel-based morphometry study. *International Journal of Clinical and Experimental Medicine*, *8*, 15383–15392.

SUPPORTING INFORMATION

Additional supporting information may be found online in the Supporting Information section at the end of this article.

How to cite this article: Suo, X., Lei, D., Li, N., Li, J., Peng, J., Li, W., Yang, J., Qin, K., Kemp, G. J., Peng, R., & Gong, Q. (2021). Topologically convergent and divergent morphological gray matter networks in early-stage Parkinson's disease with and without mild cognitive impairment. *Human Brain Mapping*, *42*(15), 5101–5112. https://doi.org/10.1002/hbm.25606